

On the Use of Fourier Methods in the Analysis of Composite Structures

BY IVANA CISAROVA, KAREL MALY AND VACLAV PETRICEK

*Institute of Physics, Czechoslovak Academy of Science, Cukrovarnicka 10,
16200 Praha 6-Stresovice, Czechoslovakia*

AND PHILIP COPPENS

Chemistry Department, State University of New York at Buffalo, Buffalo, New York 14214, USA

(Received 14 April 1992; accepted 7 September 1992)

Abstract

Different types of Fourier synthesis for composite structures are discussed. They include the two-dimensional projection based on the reflections common to both sublattices, the three-dimensional projection, which shows the average structure of one sublattice and the projection down a main (external) axis of the second sublattice, and the full four-dimensional Fourier synthesis. The three-dimensional projection includes the internal coordinate of one of the sublattices and therefore gives direct information on the nature of the modulation. The use of Fourier methods in the solution of the average structure and the analysis of the modulations is discussed. Series-termination effects are shown to affect the height of the atom strings along the internal t coordinate.

Introduction

Though the use of Fourier methods in structure refinement has diminished, Fourier methods are extensively used in structure solution and for interpretive studies, in particular in the charge density field. For conventional crystals with three-dimensional translational symmetry, the application of Fourier methods is relatively straightforward. For aperiodic crystals, appropriately described in superspace (de Wolff, 1974; de Wolff, Janssen & Janner, 1981; Janner Janssen & de Wolff, 1983), Fourier methods are less well developed. They include modulated crystals and composite crystals in which two or more lattices representing two different components coexist in the same crystal space. The use of Patterson methods in the analysis of modulated crystals has been discussed by Steurer (1987). Fourier methods were used to examine the nature of the Bi- and O-atom modulations in the 2212 high- T_c superconductor (Petricek, Gao, Lee & Coppens, 1990). Fourier methods also have important applications in the study of composite crystals defined by the coexistence of two or more sublattices in one crystal. We describe here their use in the initial structure solution and the

analysis of displacive modulations resulting from the mutual interaction between the sublattices.

Classification of composite structures

Composite structures are subject to the requirement that the two interpenetrating lattices coexist in the same space (Petricek, Maly, Coppens, Bu, Cisarova & Frost-Jensen, 1991). For a two-sublattice composite crystal, the relation between the two lattices is described by an *interlattice matrix* σ and its reciprocal-space equivalent σ^* , such that

$$A^{(2)} = \sigma A^{(1)} \quad (1)$$

and

$$A^{(2)*} = \sigma^* A^{(1)*}, \quad (2)$$

where $A^{(i)}$ and $A^{(i)*}$ are direct and reciprocal bases of lattice (i), respectively. Composite structures can be divided into *column composite structures*, in which the two lattices consist of parallel columns, and *layer composite structures*, in which sheets of the two components are interleaved. In the former case, the interlattice matrices are of the forms (Petricek *et al.*, 1991)

$$\sigma = \begin{bmatrix} \sigma_{11} & 0 & \sigma_{13} \\ 0 & \sigma_{22} & \sigma_{23} \\ 0 & 0 & \sigma_{33} \end{bmatrix}, \quad (3)$$

$$\sigma^* = \begin{bmatrix} 1/\sigma_{11} & 0 & 0 \\ 0 & 1/\sigma_{22} & 0 \\ -\sigma_{13}/(\sigma_{11}\sigma_{33}) & -\sigma_{23}/(\sigma_{22}\sigma_{33}) & 1/\sigma_{33} \end{bmatrix}. \quad (4)$$

Since σ_{11}^* and σ_{22}^* are restricted by the space-filling requirement to be integers, a basis of four reciprocal vectors, \mathbf{a}_1^* , \mathbf{b}_1^* , \mathbf{c}_1^* and $\mathbf{c}_2^* = [-\sigma_{13}/(\sigma_{11}\sigma_{33})]\mathbf{a}_1^* + [-\sigma_{23}/(\sigma_{22}\sigma_{33})]\mathbf{b}_1^* + (1/\sigma_{33})\mathbf{c}_1^*$ is sufficient to describe any diffraction vector (\mathbf{Q}) with integer indices h , k , l and m :

$$\mathbf{Q} = h\mathbf{a}_1^* + k\mathbf{b}_1^* + l\mathbf{c}_1^* + m\mathbf{c}_2^*.$$

For layer composite structures, the σ^* matrix corresponds in general to a five-dimensional description

(Petricek *et al.*, 1991). Since, in the large majority of cases, further restrictions exist that render the layer structures four dimensional, we will concentrate here on the four-dimensional case, though the methods can be extended in a straightforward manner to higher-dimensional structures.

Modulation and reflection types

The mutual interaction between the sublattices corresponds to a perturbing potential, giving rise to modulations of each of the sublattices and the appearance of satellite reflections in the diffraction pattern. For the sublattice relation described by (3) and (4), the wave vector \mathbf{q}_1 of the modulation of the sublattice 1 is equal to the reciprocal-lattice vector \mathbf{c}_2^* of the sublattice 2, while \mathbf{c}_1^* is the modulation vector for the sublattice 2. It follows that there are two contributions to the intensity of a reflection $hklm$. If either l or m equals zero, the reflection is a main reflection of lattice 2 or lattice 1, respectively, and at the same time an m th- or l th-order satellite, respectively, of the other lattice. If both m and l equal zero ($hk00$), the reflection is a main reflection of both lattices; if neither of the indices are zero, it is a satellite reflection of both lattices. For example, a reflection $hkl0$ is both a main reflection of sublattice 1 and the l th satellite of the $hk00$ reflection of sublattice 2. Thus, the reflections can be divided into main-main, main-satellite and satellite-satellite reflections.

Types of Fourier syntheses

As before, we assume the $\mathbf{a}^*\mathbf{b}^*$ plane to be the common reciprocal plane, with indices h and k . Several types of Fourier syntheses can be distinguished.

(i) *Main-main summation: two-dimensional projection based on $hk00$ reflections.* Since the $hk00$ reflections are pure main reflections for both lattices, the $hk00$ summation shows both substructures projected along the common c_1 and c_2 axes. Thus, the atoms of both substructures appear at their average position but smeared out over the modulation displacements in directions perpendicular to the c axes.

(ii) *Main-satellite summation: three-dimensional projection based on $hkl0$ or $hk0m$ reflections.* The map based on the $hkl0$ reflections is a projection of both substructures along c_2 . Since \mathbf{c}_2^* is the modulation vector of the substructure 1 and \mathbf{c}_2 the lattice translation of substructure 2, atoms of substructure 1 appear smeared out at their average positions, while those of the substructure 2 are represented by strings along c_1 projected down the c_2 axis of the substructure. This synthesis can be used to obtain the average position of the atoms of substructure 1 for input into a least-squares refinement; it also provides information on the nature of the modulations of the atoms of the substructure 2 and *vice versa* for the summation based

on the $hk0m$ reflections. The great advantage of this summation is that the average structure provides estimates of the reflection phases (signs in the centrosymmetric case), which are then used directly in the Fourier summation to give information on the modulation.

(iii) *All-reflection summation: four-dimensional Fourier synthesis.* The four-dimensional cell can be based on either substructure 1 or substructure 2 as the 'primary' lattice. The atoms of the primary lattice will appear as strings perpendicular to the three-dimensional space $R3$, those of the secondary lattice as strings parallel to the axis c^{4d} in the fourth dimension (van Smaalen, 1991). The four-dimensional Fourier synthesis provides information on the positional and modulational parameters of all atoms. Prior information on the modulation of the atoms is required for the phases of the satellite-satellite reflections ($hklm$, $l \neq 0$, $m \neq 0$).

Examples

The composite structures of $\text{Hg}_{0.776}\text{ET}(\text{SCN})_2$ [ET = BEDT-TTF = 3, 4; 3', 4'-bis(ethylenedithio)-2, 2', 5, 5'-tetrathiafulvalene] (Wang, Beno, Carlson, Thorup, Murray, Porter, Williams, Maly, Bu, Petricek, Cisarova, Coppens, Jung, Whangbo, Shirber & Overmyer, 1991) and $(\text{BO})_{2.4}\text{I}_3$ [BO = BEDO-TTF = 3, 4; 3', 4'-bis(ethylenedioxy)-2, 2', 5, 5'-tetrathiafulvalene] (Cisarova, Maly, Bu, Frost-Jensen, Sommer-Larsen & Coppens, 1991) are used for illustration purposes. The crystallographic information is as follows: * $\text{Hg}_{0.776}\text{ET}(\text{SCN})_2$: ET + SCN, $a = 6.746$ (2), $b = 20.580$ (3), $c = 4.114$ (1) Å, $\alpha = 83.06$ (1), $\beta = 119.01$ (2), $\gamma = 105.93$ (2)°, $V_c = 480.23$ Å³, $Z = 1$; Hg, $a = 6.758$ (2), $b = 21.352$ (6), $c = 5.302$ (2) Å, $\alpha = 73.10$ (2), $\beta = 119.17$ (3), $\gamma = 110.44$ (3)°, $V_c = 618.85$ Å³, $Z = 1$. The σ matrix defined by $\mathbf{A}_{\text{Hg}} = \sigma \mathbf{A}_{\text{ET+SCN}}$ is given by

$$\begin{bmatrix} 1 & 0 & -0.0077 \\ 0 & 1 & 0.9083 \\ 0 & 0 & 1.2903 \end{bmatrix}$$

indicating that the c axes of the two sublattices are parallel. The ratio of the two unit-cell volumes $V(\text{ET} + \text{SCN})/V(\text{Hg})$ is $480.23/618.85 = 0.776$, in agreement with the analytical results on the composition.

$(\text{BO})_{2.4}\text{I}_3$: BO, $a = 5.3269$ (1), $b = 16.885$ (2), $c = 4.029$ (1) Å, $\alpha = 88.29$ (2), $\beta = 81.21$ (2), $\gamma = 83.45$ (1)°; I, $a = 5.840$ (1), $b = 17.115$ (2), $c = 9.620$ (2) Å, $\alpha = 99.55$ (1), $\beta = 115.67$ (1), $\gamma = 80.19$ (1)°. The c axes of the two component structures

* Since $hk00$ is taken as the common reciprocal plane, the b and c axes of the original publications have been interchanged.

are parallel, while \mathbf{a}_1 is in the plane of \mathbf{a}_{BO} and \mathbf{c}_{BO} and \mathbf{b}_1 is in the plane of \mathbf{b}_{BO} and \mathbf{c}_{BO} , as is evident from the σ matrix defined by $\mathbf{A}_{\text{BO}} = \alpha \mathbf{A}_1$,

$$\begin{bmatrix} 1 & 0 & 0.3476 \\ 0 & 1 & 0.3476 \\ 0 & 0 & 0.4188 \end{bmatrix}$$

The component cell volumes have a ratio $V(\text{I})/V(\text{BO})=2.4$, implying the stoichiometry $(\text{BO})_{2.4}\text{I}_3$, since both subcells contain one molecule. This corresponds to an average net charge on the BO cations of $0.42e$, indicating that neutral BO molecules and BO^+ monocations coexist in the solid. The BO molecule is surrounded by linear I_3^- ions at the corners of the unit cell.

All calculations were performed by programs *JANA* and *FOURJANA* for modulated and composite structures (Petricek & Coppens, 1988; Petricek, Maly & Cisarova, 1992).

For comparison with the experimental results, a set of main and satellite reflections for $(\text{ET})\text{Hg}_{0.776}(\text{SCN})_2$ was generated using the known structure [$58\,929$ reflections up to $(\sin \theta)/\lambda = 0.7035 \text{ \AA}^{-1}$]. Isotropic temperature factors and a harmonic displacive modulation of the Hg atom (substructure 2) and the ET and SCN^- groups (substructure 1) were used, with displacements directed along the a axes of the lattices. Phases of the reflections

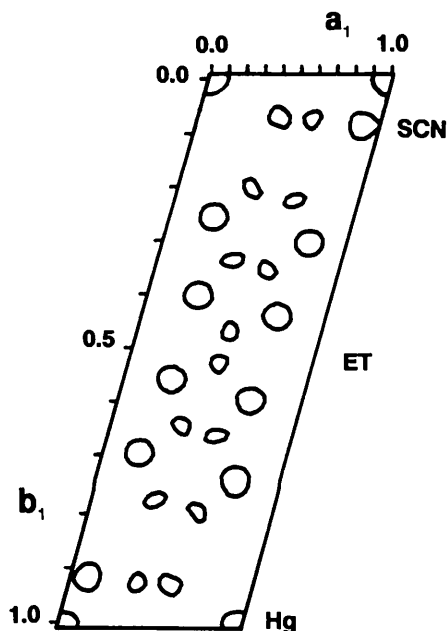


Fig. 1. The two-dimensional Fourier synthesis (0.7 e\AA^{-2} contour level only) for $(\text{ET})\text{Hg}_{0.776}(\text{SCN})_2$ based on $hk00$ reflections and model structure (see text). The peaks at average positions of all the atoms are evident. The ET molecule is in the center of the cell, the Hg atoms are at the corners and are coordinated by the SCN^- ions.

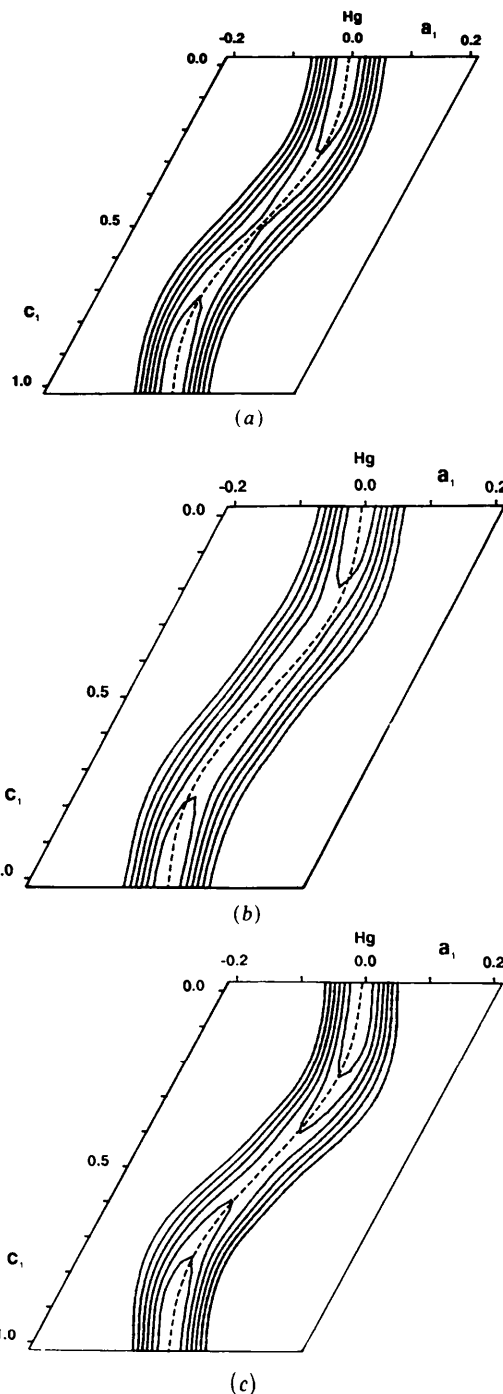


Fig. 2. Section at $y=0.0$ of the three-dimensional Fourier projection of $(\text{ET})\text{Hg}_{0.776}(\text{SCN})_2$ based on $2810 \text{ } hk00$ reflections. Contour interval 5 e\AA^{-3} , negative contours omitted. Model data with small amplitude of modulation of substructure 1. (The a -direction amplitude of the modulation of the ET molecules is taken as 0.07 \AA .) The phases of reflections have been calculated with different models: (a) both substructures and modulation of all atoms included; (b) based on average positions of atoms in both substructures only; (c) average positions of atoms of substructure 1 only, atoms of substructure 2 omitted. The 'correct' modulation function of Hg (with amplitude = 0.24 \AA) is displayed by the dashed line.

were based on either the average or the modulated positions of the atoms, as indicated below.

The summation based on the common (main-main) $hk00$ reflections, with phases based on the Hg and S positions only, is shown in Fig. 1. The $\text{ET}^{0.5+}$, SCN^- and Hg^{2+} ions can be clearly distinguished. This projection gives information on the structure, which can be used in the subsequent analysis of the interaction between the sublattices.

Examples of a section of the three-dimensional density are given in Figs. 2–5. They are based on the $hkl0$ reflections, corresponding to a space containing the average structure of component 1 (ET+SCN), but a projection down the c axis of component 2 (Hg). The a_1c_1 section shown contains the t -coordinate axis of sublattice 2 and thus shows the Hg-atom string parallel to this axis.

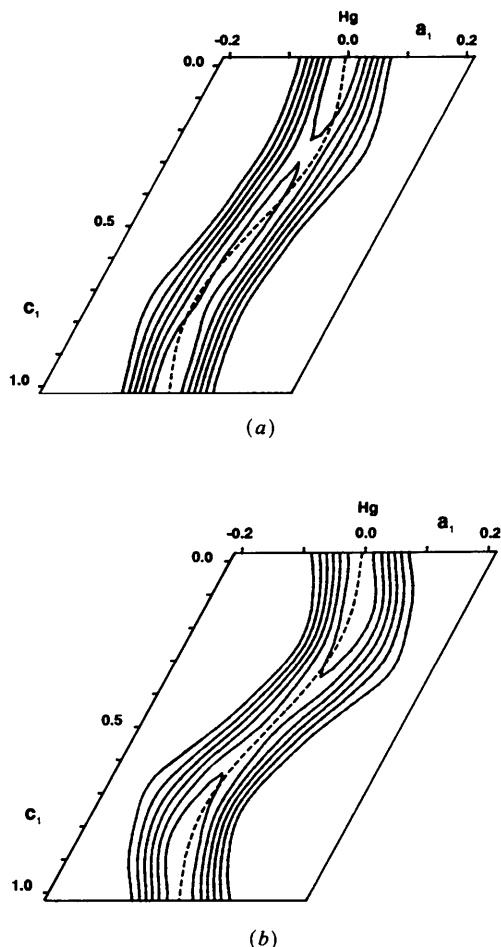


Fig. 3. Section at $y=0.0$ of the three-dimensional Fourier projection based on 2810 $hkl0$ reflections. Contours as in Fig. 2(a). Model data with large amplitude of the modulation of substructure 1 (0.34 \AA in the a direction). The models for generating phases of reflections correspond to (a) average positions of all atoms (as in Fig. 2b); (b) average positions of atoms of substructure 1 only (as in Fig. 2c).

This synthesis makes it possible to obtain information on the modulation of one of the lattices by using knowledge of the average structure of the other component. If the structure is completely known the modulation will be accurately depicted (Fig. 2a). If only the average structures are known, information on the modulation is still obtained as illustrated in Figs. 2(b) and (c), in which the phases are based on the average structure. Similar results for a larger modulation amplitude of substructure 1 are shown in Figs. 3(a) and (b) (phases based on average structure). The differences between Figs. 2(a) and (c) and 3(a) and (b) show the effect of making a large approximation (*i.e.* neglect of all of substructure 2 and the modulation of substructure 1) in the calculation of the phases. Nevertheless, the picture obtained is still qualitatively correct.

An experimental result for the same structure is given in Fig. 4, for which all structural information

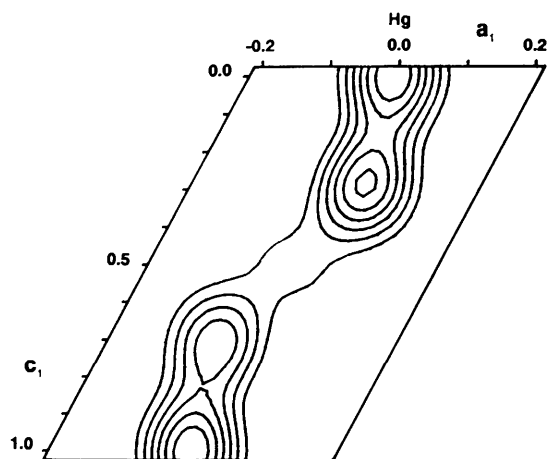


Fig. 4. Three-dimensional Fourier synthesis based on experimentally measured reflections of $\text{Hg}_{0.776}\text{ET}(\text{SCN})_2$. (Section at $y=0.0$; contour interval 5.6 e\AA^{-3} ; only positive contours are indicated.)

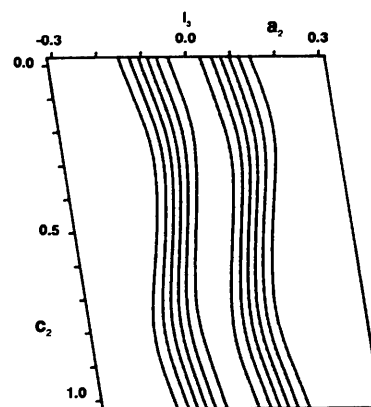


Fig. 5. Three-dimensional Fourier synthesis based on experimentally measured reflections of $(\text{BO})_2\text{A}1_3$. (Section at $y=0.0$; contour interval 8.6 e\AA^{-3} ; only positive contours are indicated.)

was included in the phase calculation. It is clear that the modulation is quite anharmonic and much more like a step function than was realized in the original analysis, which was based only on least-squares methods. A similar two-dimensional section of the three-dimensional $hkl0$ projection of $(\text{BO})_{2.4}\text{I}_3$, based on experimental data, is shown in Fig. 5. As the I_3^- ion is aligned along the c axis, the three I atoms superimpose in this c -axis projection.

Series-termination effects

In the ideal case of a pure displacive modulation with a nonmodulated temperature parameter, the string will have equal peak height and width in every three-dimensional section perpendicular to the t axis [Fig. 6(a), based on all model structure factors]. However, the shape of the atom string is very sensitive to the completeness of the data set. The experimental data set, F_{hklm}^{exp} is given by

$$F_{hklm}^{\text{exp}} = G_{hklm} F_{hklm}^{\infty},$$

where F_{hklm}^{∞} is the complete set of structure factors and G_{hklm} is the reciprocal-space shape function describing the truncation of the data set (Hoseman & Bagchi, 1962). The shape function for a set of data with only first-order satellites is truncated along the direction of the satellite index. When the Hg modulation is considered, this is the l index,

$$G_{hklm} = \begin{cases} 1 & \text{for } |l| \leq 1, \\ 0 & \text{for } |l| > 1. \end{cases}$$

From the Fourier-convolution theorem, the experimental electron density of a crystal is a convolution of the Fourier transform of G_{hklm} and the ideal electron density given by the Fourier transform of a complete set of F_{hklm}^{∞} . The effect of incompleteness of a data set may be illustrated by a plot of the function $\hat{F}(G_{hklm})$, where \hat{F} is the Fourier-transform operator. Fig. 6(b) shows $\hat{F}(G_{hklm})$ for an extensive data set, sufficient to produce a close-to-ideal modulation string (Fig. 6a). Maps of $\hat{F}(G_{hklm})$ and $\hat{F}(F_{hklm}^{\text{exp}})$ for the frequently encountered case of data with only first-order satellites are shown in Figs. 7(a) and (b). The modulation string follows the modulation curve of the model but its height and width vary along the t coordinate. The size of the deformation depends on the relative directions of the anisotropy of $\hat{F}(G_{hklm})$ and the modulation string. Fig. 7 represents the worst case of the deformation since the large smearing of $\hat{F}(G_{hklm})$ is parallel to the t axis.

Unlike in the difference Patterson function (DPF) defined by Steurer (1987), the main reflections were included in the syntheses shown here to make the

comparison with the ideal electron density maps more straightforward. As an experimental data set sufficiently complete to eliminate series-termination effects is often not available, the difference Fourier synthesis may be preferable for the study of details such as the temperature-factor modulation or the

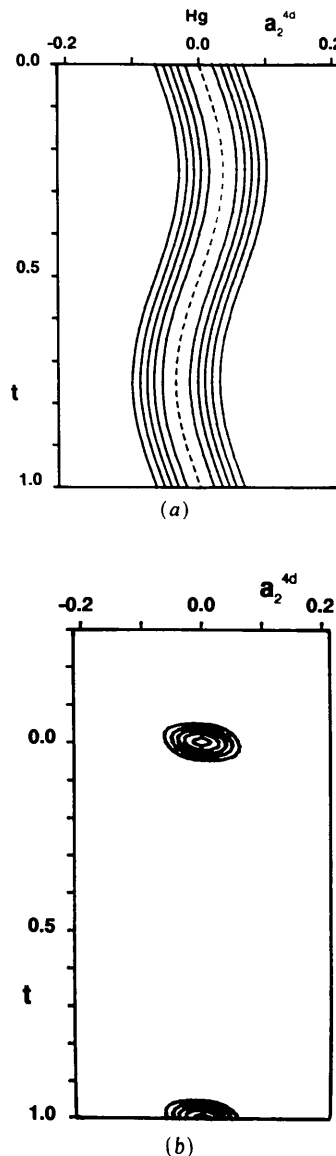
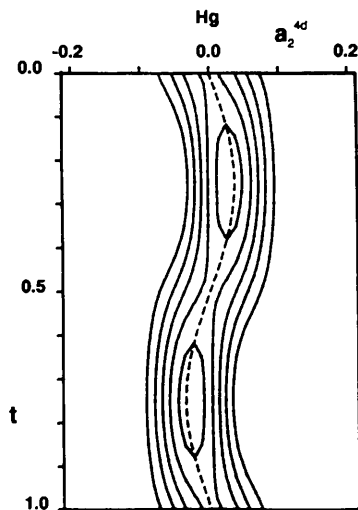
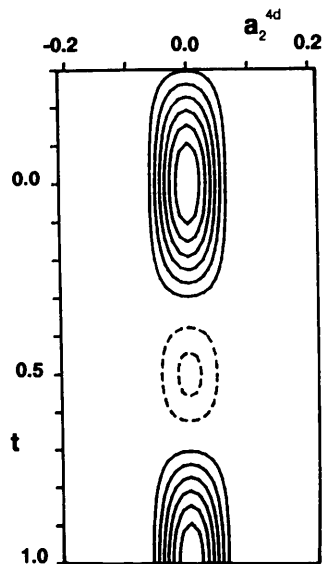


Fig. 6. (a) The four-dimensional Fourier synthesis from 58 929 $hklm$ reflections (section at $y^{4d} = 0.0$, $z^{4d} = 0.0$) of $\text{Hg}_{0.776}\text{ET}(\text{SCN})_2$. The modulation string of the Hg atom in substructure 2 is indicated by the broken line. In this and the following figures, the primary cell is taken as the Hg cell, the a_2^{4d} axis is the four-dimensional axis corresponding to $a(\text{Hg})$ (the a_2^{4d} and t directions are almost but not exactly perpendicular to each other). (b) The four-dimensional Fourier synthesis of the shape function for a sphere with radius $(\sin \theta)/\lambda = 0.7035 \text{ \AA}^{-1}$ containing 58 929 main and satellite reflections of $\text{Hg}_{0.776}\text{ET}(\text{SCN})_2$ (satellite index < 15) (section at $y^{4d} = 0.0$, $z^{4d} = 0.0$).



(a)



(b)

Fig. 7. (a) Section ($y^{4d} = 0.0$, $z^{4d} = 0.0$) of the four-dimensional Fourier synthesis of $\text{Hg}_{0.776}\text{ET}(\text{SCN})_2$. Contours as in Fig. 6. Experimental data containing first-order satellites only. Maxima occurring in the string are due to series-termination effects. (b) The four-dimensional Fourier synthesis of the shape function for a sphere with radius $(\sin \theta)/\lambda = 0.7035 \text{ \AA}^{-1}$ containing only 10 880 main and satellite reflections with $|l| \leq 1$ of $\text{Hg}_{0.776}\text{ET}(\text{SCN})_2$ ($y^{4d} = 0.0$, $z^{4d} = 0.0$). Contours as in Fig. 6.

combination of displacive and occupational modulations.

Concluding remarks

The $hkl0$ and $hk0m$ three-dimensional-projection syntheses are unusual in that they give direct information on the modulation from a knowledge of the average structures or even one of the average structures only. Information from these main-satellite summations can be used in an iterative procedure to recalculate the phases for the next Fourier summation. The example of the Hg modulation in $\text{Hg}_{0.776}\text{ET}(\text{SCN})_2$ shows that nonharmonic modulation functions, which may be overlooked in an analysis based exclusively on least-squares methods, can be recognized by use of such a summation.

Support of this work by the National Science Foundation (CHE9021069) and the Petroleum Research Fund administered by the American Chemical Society (PRF21392-AC6-C) is gratefully acknowledged.

References

- CISAROVA, I., MALY, K., BU, X., FROST-JENSEN, A., SOMMERLARSEN, P. & COPPENS, P. (1991). *Chem. Mater.* **3**, 647-651.
 HOSEMAN, R. & BAGCHI, S. N. (1962). *Direct Analysis of Diffraction by Matter*, pp. 198-203. Amsterdam: North-Holland.
 JANNER, A., JANSSEN, T. & DE WOLFF, P. M. (1983). *Acta Cryst.* **A39**, 658-666.
 PETRICEK, V. & COPPENS, P. (1988). *Acta Cryst.* **A44**, 235-239.
 PETRICEK, V., GAO, Y., LEE, P. & COPPENS, P. (1990). *Phys. Rev.* **B42**, 387-392.
 PETRICEK, V., MALY, K. & CISAROVA, I. (1992). *Methods of Structural Analysis of Modulated Structures and Quasicrystals*, pp. 262-268. Singapore: World Scientific.
 PETRICEK, V., MALY, K., COPPENS, P., BU, X., CISAROVA, I. & FROST-JENSEN, A. (1991). *Acta Cryst.* **A47**, 210-216.
 SMAALEN, S. VAN (1991). *Phys. Rev. B*, **43**, 11330-11341.
 STEURER, W. (1987). *Acta Cryst.* **A43**, 36-42.
 WANG, H. H., BENO, M. A., CARLSON, K. D., THORUP, N., MURRAY, A., PORTER, L. C., WILLIAMS, J. M., MALY, K., BU, X., PETRICEK, V., CISAROVA, I., COPPENS, P., JUNG, D., WHANGBO, M.-H., SHIRBER, J. E. & OVERMYER, D. L. (1991). *Chem. Mater.* **3**, 508-513.
 WOLFF, P. M. DE (1974). *Acta Cryst.* **A30**, 777-785.
 WOLFF, P. M. DE, JANSSEN, T. & JANNER, A. (1981). *Acta Cryst.* **A37**, 625-636.